Stars and planets at high spatial and spectral resolution

Albrecht, S.

Chapter 6

Ground based transmission spectroscopy of the atmosphere of HD 209458b using the VLT

Recently, Snellen et al. (2008) have presented the ground-based detection of sodium in the transmission spectrum of the extrasolar planet HD 209458b. They showed that under good atmospheric circumstances and with the right observing strategy and analysis methods, ground-based transmission spectroscopy of exoplanets can lead to detections. The aim of this chapter is to show that the sodium absorption also appears in another ground-based data set, that transmission spectroscopy can be done routinely from the ground, and to target, besides sodium, also potassium in the atmosphere of HD 209458b. We carried out ground-based transmission spectroscopy of HD 209458b using the UVES spectrograph at Kueyen (Unit Telescope 2) of the Very Large Telescope at the Paranal Observatory. The obtained spectra have been corrected for instrumental effects which influence the transmission spectroscopy, such as a change of the blaze function of the spectrograph, and a non linearity effect in the CCD. Furthermore the influence of telluric sodium absorption, and absorption due to water in earth's atmosphere has been corrected for in the spectra. Although the first part of the transit was missed due to technical problems, and the weather was less stable than during the Snellen et al. (2008) observations, we also detect sodium. Our measurements are fully consistent with earlier results. We further extend these observations by measuring the ratio between the Na D_2 and Na D_1 lines to be ~ 1.8. Around the centre of the transit the planetary sodium absorption seems to be less deep than during the rest of the transit, of which a hint is also seen in the Snellen et al. (2008) data. If real, this could be caused by the change in relative radial velocity of the planet with respect to that of the star, with the planets absorption centered at the heart of the stellar absorption line during mid-transit. For absorption by potassium in the atmosphere of HD 209458b, we find an upper 3-σ limit of 0.042% in a passband of 1.5Å.

S. Albrecht & I.A.G. Snellen
A&A to be submitted

6.1 Introduction

A stellar spectrum observed through the atmosphere of a transiting planet carries the spectral imprint of the atomic and molecular species in that atmosphere, making the depth of the transit wavelength dependent. Comparing in-transit with out-transit spectra of the host star can therefore reveal information about the composition and structure of the planet's atmosphere (e.g. Seager & Sasselov 2000) which would otherwise remain inaccessible. This opens the fascinating possibility to study the physical and chemical characteristics of these alien atmospheres. For hot Jupiters two prominent absorption features are expected caused by resonance lines of alkali metals in the visible wavelength band. Absorption by sodium in the Na D lines at 5889 Å and 5895 Å, and absorption by potassium in the K I lines at 7665 Å and 7699 Å (e.g. Brown 2001). Charbonneau et al. (2002) were the first to detect the sodium feature in the transmission spectrum of an extra solar planet, HD 209458b using the Space Telescope Imaging Spectrograph (STIS) on board of the Hubble Space Telescope (HST). This way, for the first time information is received about the conditions in an atmosphere of an planet orbiting a different sun. This same data set has recently been re-analyzed by Sing et al. (2008a,b), showing the presence of an additional broad absorption component. The only successful ground-based observations of an extra solar planetary atmosphere have been presented by Redfield et al. (2008) and from our group (Snellen et al. 2008). Redfield et al. (2008) detected sodium absorption by the atmosphere of HD 189733b using the Hobby-Eberly Telescope. Snellen et al. (2008) re-analyzed archival HDS/Subaru data of HD 209458 for a range of different passbands. Their findings are fully consistent with the results by Charbonneau et al. (2002) and Sing et al. (2008a).

We here continue these measurements to pursue three aims. The first goal is a further investigation of the sodium absorption by the atmosphere of HD 209458b. Second, to show that these observations can be routinely done also with the Very Large Telescope (VLT). Our final goal is to search for absorption by potassium, which is expected to produce absorption at a similar level as sodium in the atmosphere of HD 209458b. This chapter is structured as follows: In Section 6.2 we describe the observations from ESO's Paranal Observatory. Subsequently, we present our analysis and results for sodium and potassium in the sections 6.3.1 and 6.3.3. The discussion in section 6.4 is followed by our conclusions.

6.2 UVES VLT observations

On the night of August 13, 2006 we obtained 56 high resolution spectra of HD 209458 using the Ultraviolet and Visual Echelle Spectrograph (UVES, Dekker et al. 2000) on Kueyen (UT2) of the VLT. Sixteen observations were taken during, and forty after, the planetary transit. The beginning of the transit was missed partly because of bad weather and technical problems. The sky remained partly cloudy throughout the night. In Figure 6.1 the atmospheric conditions for each observation are shown. The 1D-seeing, indicated by the dashed line, is measured from the 1D stellar profile on the CCD. The strength of telluric water lines, which is arbitrary normalized and indicated by crosses, is measured by a set of strong H_2O lines. The dotted line shows the normalized continuum count level in each observation. Note the particularly low count levels for frames 17 – 20. These frames have been significantly influenced by clouds, while the integration were stopped a few times, because the telescope had lost track of the star.

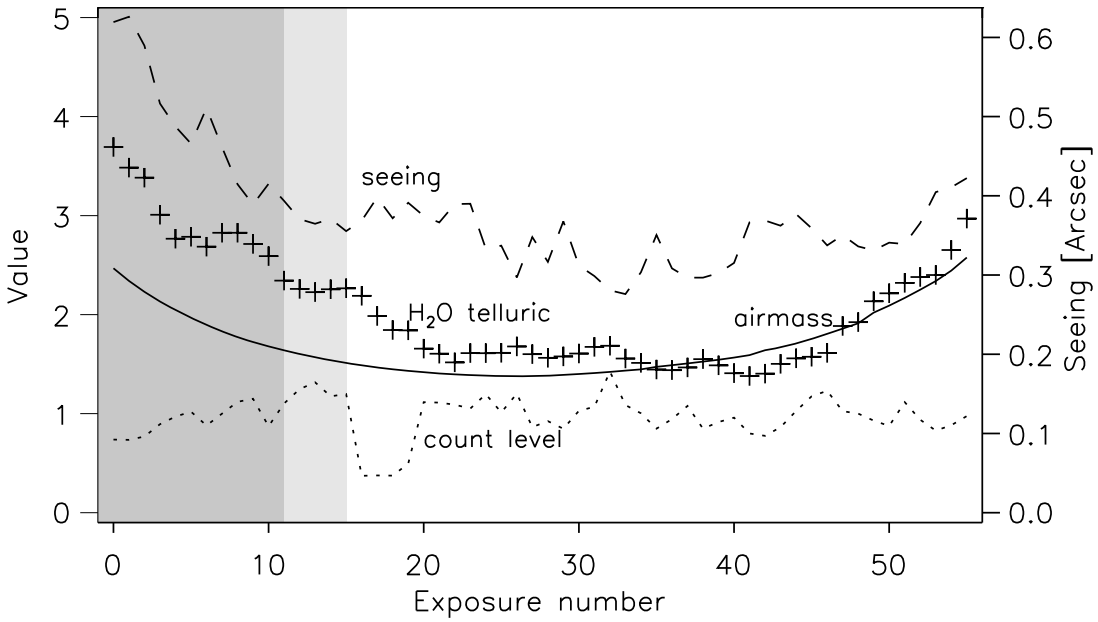

Figure 6.1 — The panel shows the environmental conditions during the observations of HD 209458 at the VLT in the night 13/14 August 2006. The grey areas indicate the timing of the planetary transit and period of egress. The solid line indicates the airmass for which HD 209458b was observed, and the dotted line indicates the normalized flux in the exposures. The dashed line shows the seeing (in σ) as measured from the the one-dimensional profile of the star along the slit. The crosses indicate the strength of telluric water lines.

These frames are shown here but have been excluded from the analysis.

The data were taken using a free template, with dichroic 2, and cross disperser 2 (CD2). Using a slit of 0.5 $''$, which was aligned with the parallactic angle, a resolving power of R $\sim$ 65 000 was obtained and a wavelength range of 3800 Å $< \lambda <$ 9000 Å was covered. Typical exposure times were 400 seconds, but for a few observations the exposure time was altered to account for changes in the flux level, and to achieve an as uniform as possible S/N level for each observation throughout the night. After initial data reduction, using the ESOREX (version 3.6.1) software package [1] , we extracted spectra with a S/N ratio between 200 – 300 in the continuum around the Na D lines and with a similar S/N ratio in the continuum around the K I potassium lines.

6.3 Transmission spectroscopy

The relative strength of the absorption features is determined in each reduced spectrum by integrating the flux in a wavelength band centered around the appropriate wavelength. This flux is divided by the flux in adjacent, equally wide bands on the short and long wavelength side of the central wavelength band. Differences of these ratios between in-transit and out-transit

[1] We used the -reduce.extract.profile='gauss' option for the uves_obs_scired recipe, because the default option 'virtual' to extract the orders resulted in a quasi periodic pattern, even if the resolution is chosen to be 0.1 pixel.

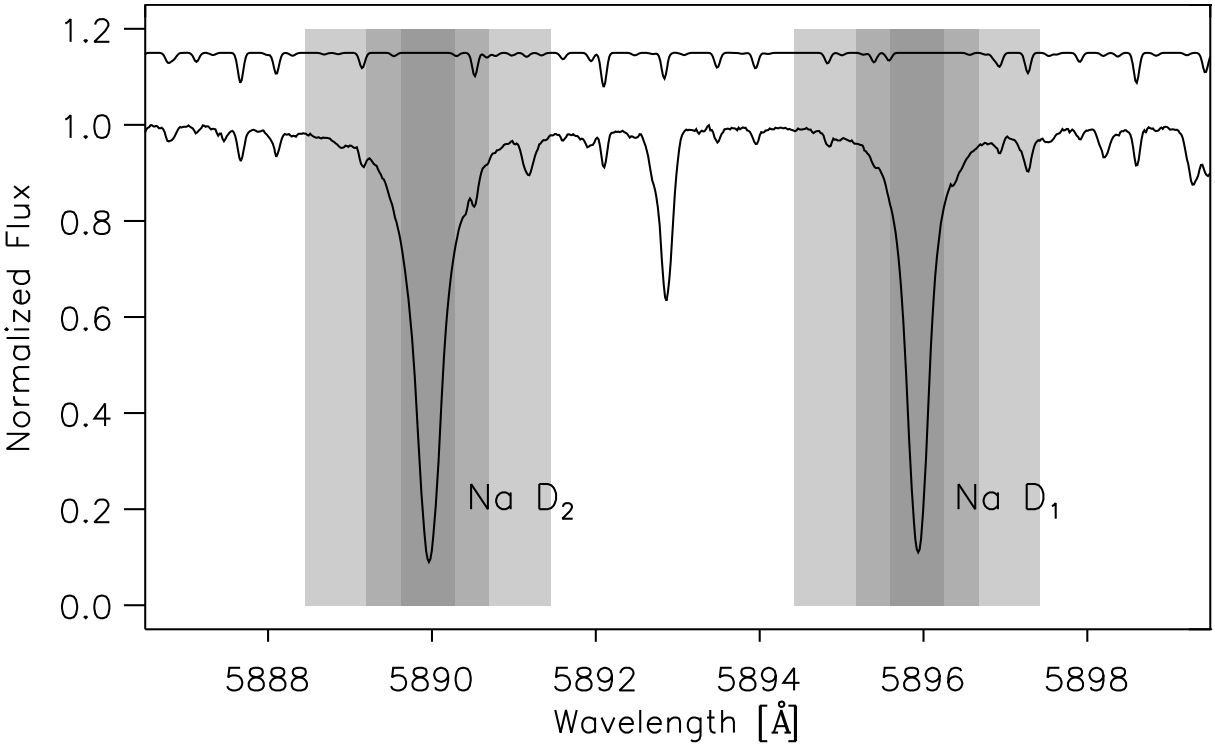

Figure 6.2 — This figure shows a spectrum of HD 209458b obtained with UVES at the UT2. The shaded regions represent three central passbands with a width of 2×0.75 Å, 2×1.50 Å, and 2×3.0 Å. The upper spectrum represents a telluric spectrum, mainly consisting of H_2O lines, created using the line list of Lundstrom et al. (1991).

spectra, are subsequently attributed to absorption:

$$\left.\begin{aligned} F_{\rm left} &= \int_{\lambda_0-\frac{3}{2}\Delta\lambda}^{\lambda_0-\frac{1}{2}\Delta\lambda} F(\lambda)d\lambda \\ F_{\rm cen} &= \int_{\lambda_0-\frac{1}{2}\Delta\lambda}^{\lambda_0+\frac{1}{2}\Delta\lambda} F(\lambda)d\lambda \\ F_{\rm right} &= \int_{\lambda_0+\frac{1}{2}\Delta\lambda}^{\lambda_0+\frac{3}{2}\Delta\lambda} F(\lambda)d\lambda \end{aligned}\right\} \quad F_{\rm line} = \frac{2F_{\rm cen}}{F_{\rm left}+F_{\rm right}} \tag{6.1}$$

where $F_{\rm cen}$, $F_{\rm left}$, and $F_{\rm right}$ are the measured fluxes in the central and two adjacent comparison bands. The center wavelength of the absorption line is indicated by λ_0, and $\Delta\lambda$ stands for the total width of each of the passbands. The flux ratios of the central to adjacent bands is indicated by $F_{\rm line}$, which should be lower during transit if absorption by the planet atmosphere is detected.

6.3.1 Sodium

We searched for absorption by sodium around the Fraunhofer D resonance lines. The exact position of the line center was determined through Lorentzian fitting for the Na D lines, and Gaussian fitting for other comparison lines. For the Na D_2 line the exact position was also determined after the change in strength of a telluric water line, which lies on the wing of the stellar line, was removed. Figure 6.2 shows the spectral region around the Na D doublet, with the three central passbands used in our and in the analysis by Snellen et al. (2008) are indicated by gray shaded areas. The passbands, used for comparison, are always located directly next to these.

Before Equation 6.1 can be used to derive the absorption of the planetary atmosphere, other effects which change with time and which influence the ratio between the central and sidebands, both instrumental and induced by the earth atmosphere, have to be excluded.

Instrumental effects

Two important instrumental effects influence our spectra. The blaze function of the spectrograph slowly changes over night and introduces a change of flux between the different bands over the time scale of a planetary transit. The use of Equation 6.1 only prevents zero or first order effects to influence the transmission spectroscopy. Any higher order effect, e.g. a change in spectral curvature of the blaze function will not be corrected for. A good way to treat the change of the blaze function in transmission spectroscopy is explained in Winn et al. (2004), has been applied by Snellen et al. (2008), and is also followed in this chapter: Fortunately, the blaze functions change only very slowly as a function of the spectral order. Therefore, one can use the change in blaze function between frames in the two adjacent orders to correct for the change in the blaze function in the order of interest, without introducing possible systematic effects due to the planetary absorption.
The second instrumental effect for which we corrected is a non-linearity in the conversion factor of the CCD and its electronics. If the conversion factor decreases slowly towards a high count level, but this is not taken into account by the reduction software, then high count levels are overestimated and low count levels are underestimated. If the count level for each exposure changes, one expects that the depth of an absorption line is underestimated for high count levels and vice versa. This effect has been first identified by Snellen et al. (2008). To quantify this effect we measured the depth of 40 deep absorption lines, for which we do not expected that planetary absorption plays a role, for each exposure in a 0.75 Å passband. Note that all these lines are located on the lower red CCD of UVES. By comparing Figure 6.3 with Snellen et al. (2008) Figure 3. one can see that the effect in our data set is a factor ~ 2 lower than in their data set. We corrected for this effect in the same way as in Snellen et al. (2008). A comparison of the corrected and uncorrected absorption depth for the 40 lines plotted as a function of exposure number can be seen in Figure 6.4.

Earth's atmosphere

For ground-based observations, one also has to correct for telluric effects. In the wavelength regions of the Na D lines, changes in the strength of telluric absorption lines, caused by H_2O and also sodium in the Earth atmosphere, can be problematic. Note that the regions in the

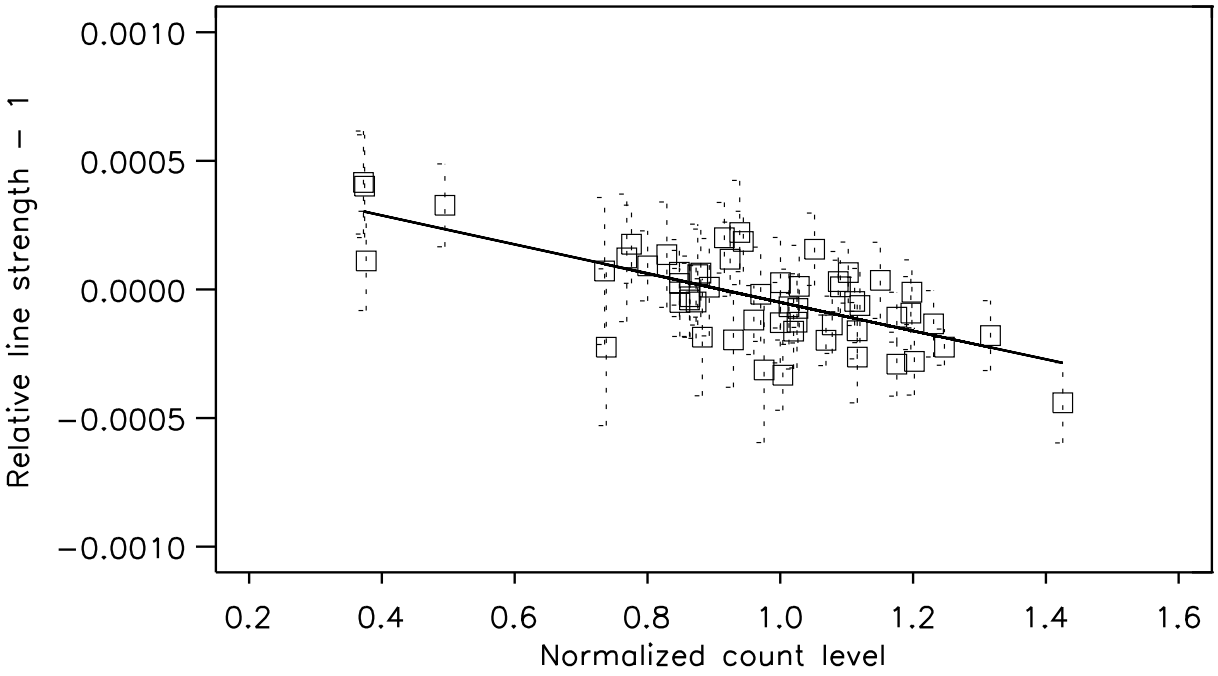

Figure 6.3 — Normalized mean line depth of 40 strong stellar lines plotted as a function of the normalized flux for the 56 exposures. A clear trend is visible, indicating that a non-linearity influences the data.

earth atmosphere where the telluric water lines and the telluric sodium absorption originate are not identical and therefore the change of these telluric features over time can differ. See figure 6.5 for a zoom in the spectral region around the stellar Na D_2 lines, where one can see the development over night of two prominent H_2O absorption lines and the telluric sodium Na D_2 line.

Telluric sodium: An important contribution of the earth's atmosphere to the observed spectra is additional sodium absorption. This absorption is, due to the relative difference in radial velocity between earth's atmosphere and HD 209458 ($\sim$ 23 km sec^{-1}) displaced by $\sim$ 0.45 Å relative to the stellar sodium lines (Figure 6.5). The development of the strength of the telluric Na D lines can therefore be measured and is shown in Figure 6.6. Clearly the change in the Na D_1 line over the night and its absolute strength are lower compared to that of the D_2 line. We corrected for the telluric sodium in the following way. First a reference spectrum was constructed from 5 frames (nr. 24 – 28) taken at low airmass. Each individual frame of the night was subsequently divided by this reference spectrum. In this way the change (not the absolute value) of the telluric sodium absorption becomes visible, which was fitted with a Gaussian fixed in position and width. This Gaussian model to the change in telluric sodium absorption was subsequently removed from the spectra to make its contribution constant with time. Variations in the D_2/D_1 ratio at Paranal are not uncommon, but have only been measured on a longer timescale, with an average line ratio of 1.6 (see Patat 2008). Our correction for the telluric sodium will hide the sodium signal of the atmosphere of HD 209458b over the wavelength range of 0.05 Å. However, as the smallest band-pass employed in this study is 0.75 Å we expect no

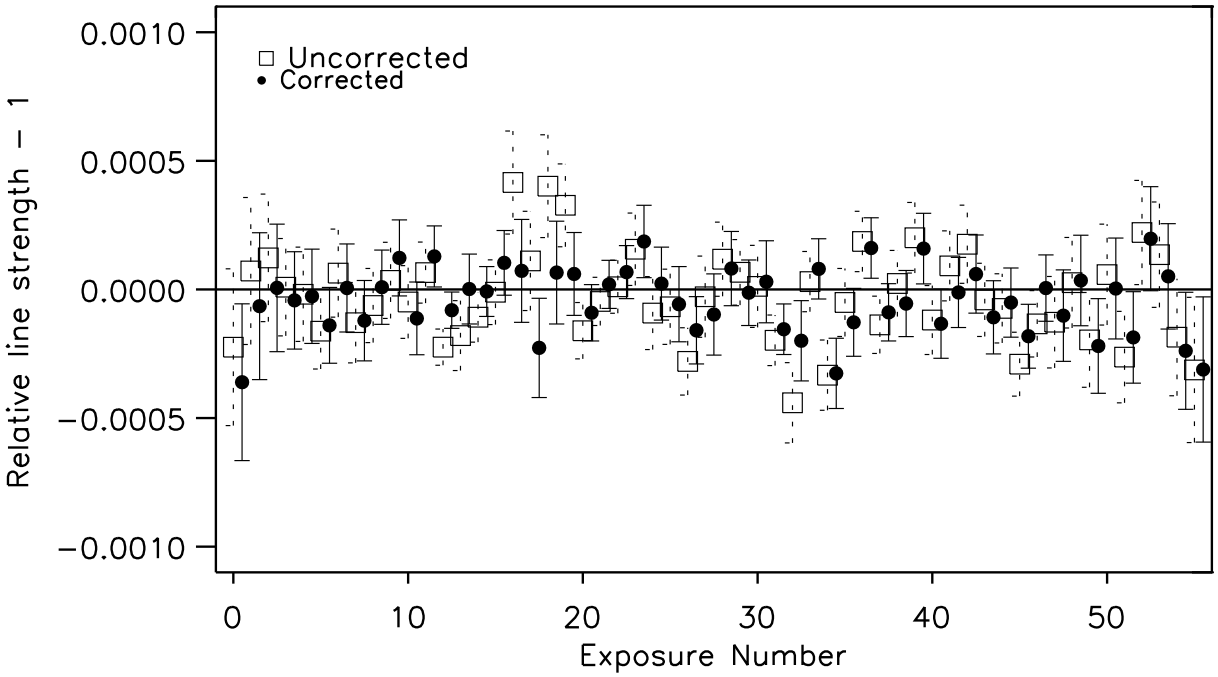

Figure 6.4 — Uncorrected (empty squares) and corrected (filled circles) average normalized mean line depth of 40 strong stellar lines plotted over the exposure number. The corrected values are shifted by 0.5 in exposure number for clarity.

significant additional error, compared to our uncertainties. Moutou et al. (2001) have noticed similar features appearing and disappearing during different exposures at similar wavelengths in their study of HD 209458b's atmosphere (their Figure 4.). Note that around the same time the telluric sodium features start to strengthen in our data set, the moon is rising above the horizon. However we think this effect is unlikely caused by reflected sunlight, since the star with $m_V = 7.65$ is so much brighter compared to the sky background. It is known that the moon has its own sodium atmosphere which extends to several times the radius of the moon and covers several degrees on the sky (see Mendillo 2001). However, HD 209458's angular distance on the sky ($\sim 50\,^\circ$) was too large for our measurements to be influenced by it, and this distance does not change over the course of one night as the sodium feature does. Most likely it is the change in weather pattern in the Earth's upper atmosphere which is responsible for the increase in the line strength of the telluric sodium absorption. For example the cloud coverage varied over night.

Water lines: The main contribution of the telluric spectrum around the Na D doublet consists of water absorption lines (see Figures 6.2 and 6.5). We measured the change in strength of strong water lines in the 7000 Å regime as a tracer for the strength of the telluric water lines around the Na D doublet, since these lines can be measured much more accurately. The crosses in Figure 6.1 show the scaled development of the mean of these absorption lines over time. We confirmed this measurement with measurements of the weaker H_2O lines around the Na D doublet, but at a higher noise level. Due to the change in weather conditions during the night, the strength of the water lines does not follow the airmass: If it had been a perfectly stable

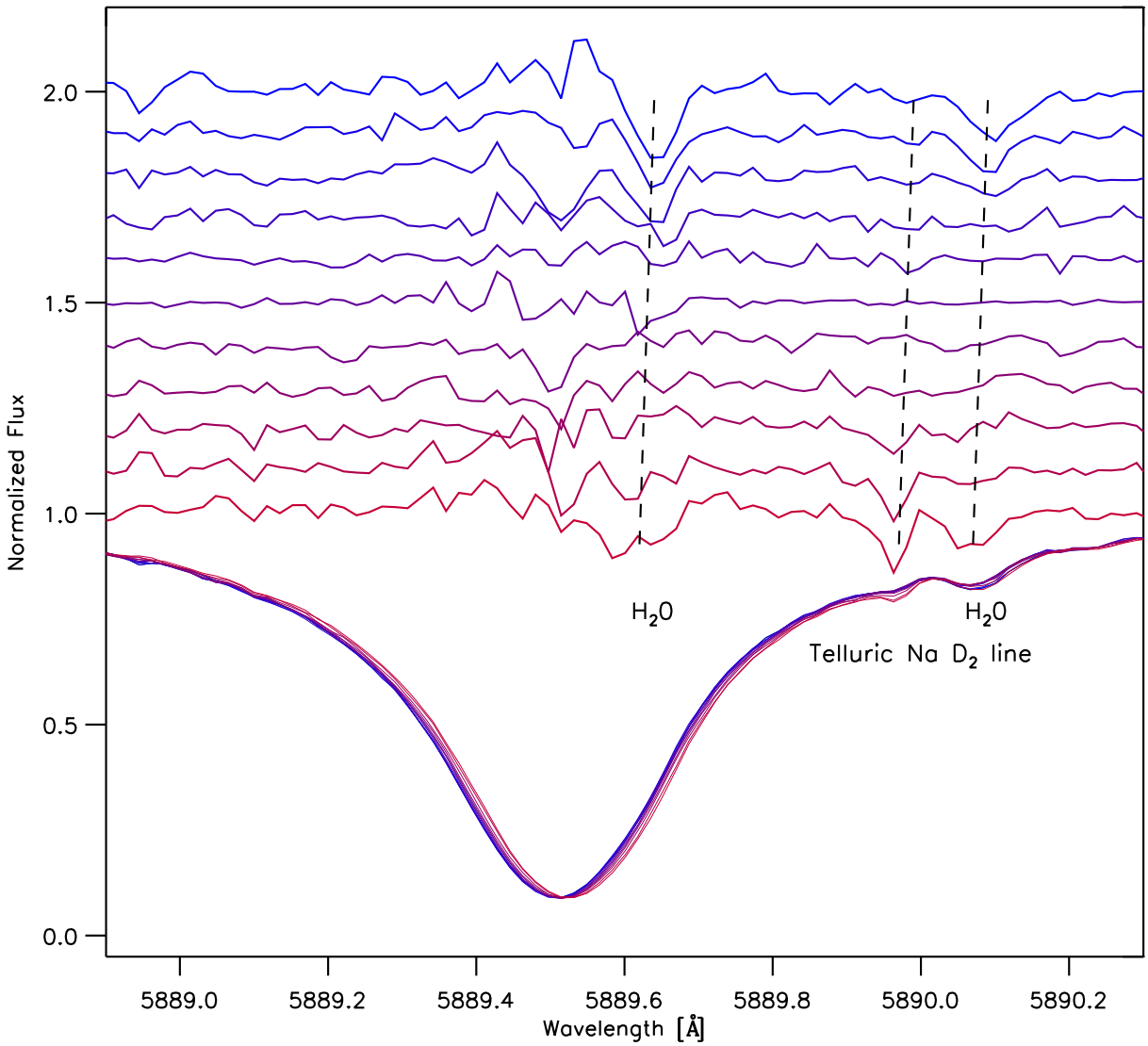

Figure 6.5 — The spectral region around the Na D_2 line. Eleven spectra are plotted as function of wavelength in the rest frame of the observatory. Each spectrum represents the median of 5 consecutive frames. One can see that the stellar absorption line shifts in wavelength space over night by ~ 0.02 Å towards longer wavelengths. The upper lines represent these median spectra divided by the median of 5 spectra obtained at low airmass (see also text) in the *stellar* rest frame. These "relative spectra" have been amplified by $\times 5$ in this plot. The median of the first five spectra obtained during the night is displayed at a flux value of 2 and each following spectrum is shifted by 0.1 units down. The wavelength position of the telluric sodium line and two strong H_2O lines are indicated. Also indicated by the slightly tilted lines is the relative shift of the telluric lines in the stellar rest frame over time due to the change in relative radial-velocity. The water lines are prominent at the begin of the night, decrease during the middle, and increase later again. The telluric sodium line does not change significantly over the first half of the night, and later increases in depth. Note that the S/N in the "relative spectra" is significantly lower in the core of the Na D_2 line as a low flux level is divided by a low flux level.

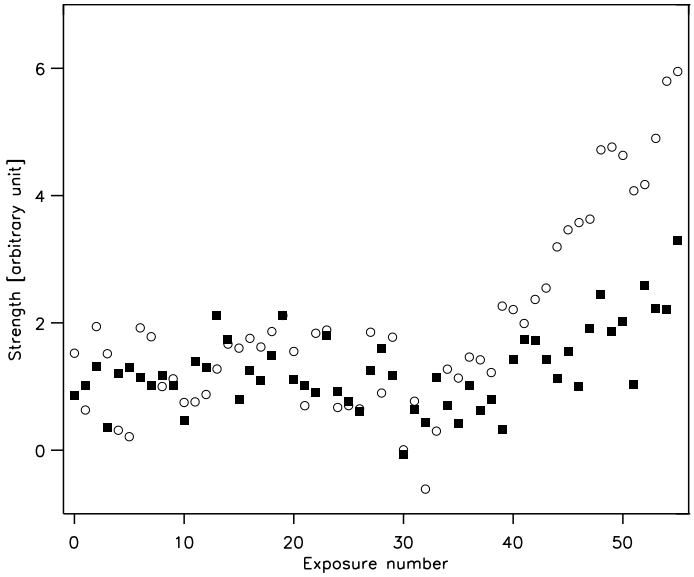

Figure 6.6 — The development of the two telluric sodium lines as a function of the exposure number. The D_1 line is represented by filled squares and the D_2 line by open circles.

night, the water column would have been constant in time, and purely a function of viewing angle, making the strength of the H_2O telluric lines follow airmass (see Snellen et al. 2008).

The change in absorption of stellar light by telluric water in the different spectra effects the data reduction and the transmission spectroscopy in two ways. Firstly, the contribution of telluric H_2O lines in the central passband will make the observed absorption appear deeper, while those lines located in the adjacent bands will make it appear shallower. It therefore depends on the distribution of H_2O lines and the size of the passbands in which way telluric H_2O lines will influence the measurements. Secondly, the telluric lines in the adjacent orders also influence the results in a indirect way, since these orders are used to correct the blaze function of the spectrograph. One can correct for both effects, after conducting the transmission spectroscopy by correlating the strength of the strong telluric water lines around 7000 Å with the measured strength of the Na D absorption outside the transit, and use the inferred coefficient to correct all spectra of the night, and afterwards find the difference in absorption depth during and out of transit. We measured the relative line strength of the sodium absorption in three passbands around the two Na D lines for passbands similar to those used by Snellen et al. (2008) and Sing et al. (2008a). See section 6.3.2 and Figure 6.8 for our results using this method.

Instead of removing the influence of the telluric water lines in the transmission spectroscopy one can also remove the change of the strength of the telluric lines in the spectra itself, before carrying out the transmission spectroscopy. For this we used the information on telluric lines in the wavelength region around the Na D doublet compiled by Lundstrom et al. (1991) to create a model telluric spectrum. Lundstrom et al. (1991) provided the wavelength positions and most importantly the relative depth of the different telluric lines. This approach has two weaknesses. The relative strengths of the different absorption lines have to be known to very high accuracy to remove all changes. Furthermore the effect mentioned above; the influence of the correction of the change of the blaze function of the spectrograph due to the water lines can not be corrected in this way. However, the advantage is that one can take into account the relative movement of the telluric lines with respect to the stellar absorption lines during the night. The radial velocity of the star changed, mainly due to acceleration of the observatory relative to the star, by nearly 1km $\sec^{-1}$, equivalent to a shift of ~ 0.02 Å at 6000 Å (see also Figure 6.5). Therefore keeping

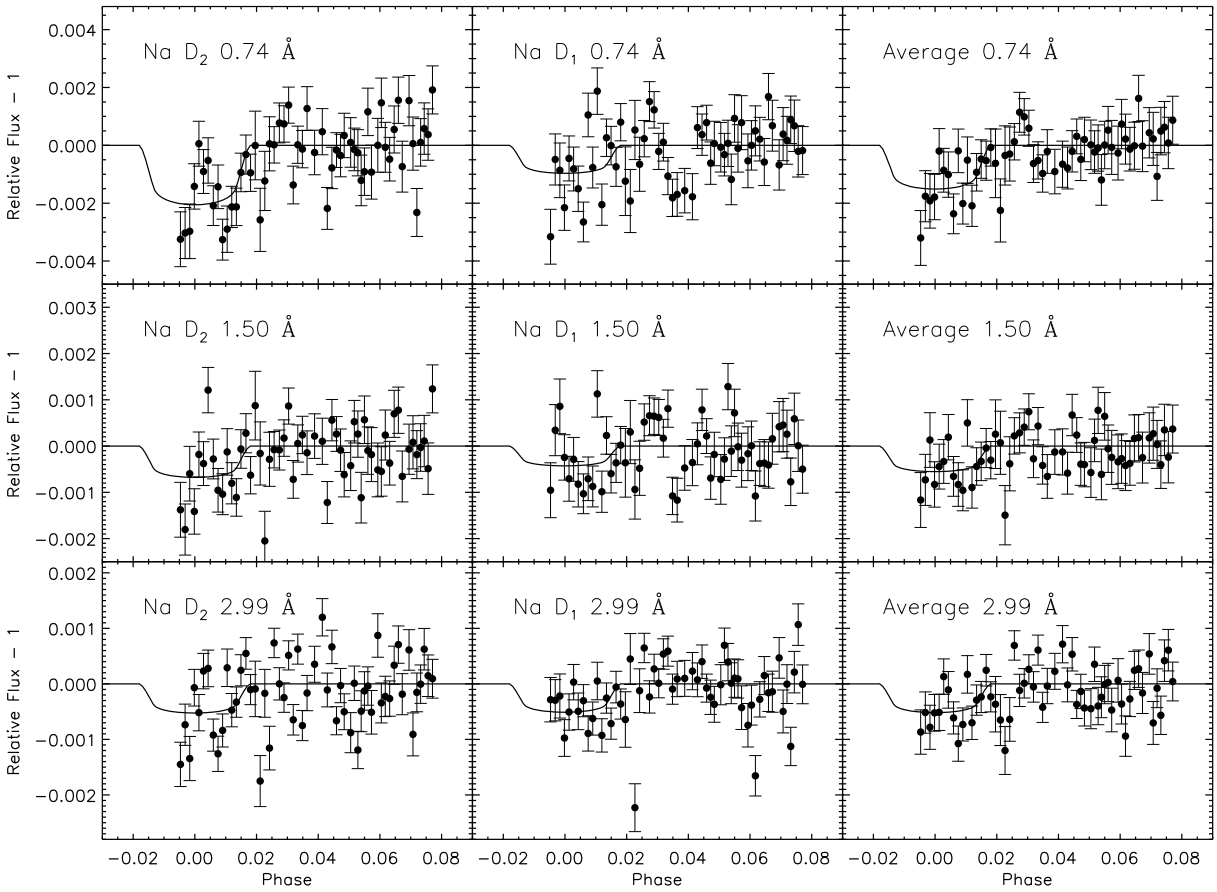

Figure 6.7 — The left panels show the sodium absorption in the Na D_2 line for the three different passbands of 0.75 Å, 1.5 Å, and 3.0 Å, in the top, middle, and bottom panel, respectively. The middle panel show the same for the Na D_1 line and the right panels for the average of the two. The solid line represents our best fit.

the passbands fixed in the rest frame of the star can mean that a telluric line is moving partly from one passband into an adjacent passband over the course of the night (see also section 6.3.3 and the Figures 6.9 and 6.10). This is not taken care of in the first method used in this work. It turns out that for the chosen passbands of 0.75 Å, 1.5 Å, 2.2 Å, and 3 Å around each sodium line no significant telluric line lies at a border of one of the passbands. Hence this effect does not influence the measured absorption due the planetary atmosphere. However, if transmission spectroscopy is conducted at many different passbands this effect is indeed important in our data set and first the synthetic spectra of telluric lines have to be subtracted from each observation, scaling it to the overall depth of the telluric features in that observation. This way the change in the telluric lines over time is removed to a high degree and the absorption due to HD 209458b's atmosphere can be calculated at different passbands. A final correction for the telluric features is still needed in the transmission spectroscopy due to residuals in the removal of the telluric lines and the influence the change of the telluric lines has on the blaze correction. Furthermore, we did not remove the change in the strength of the telluric water line located in the core of the Na D_2 line (only to derive its exact position in wavelength). Due to the low flux and the

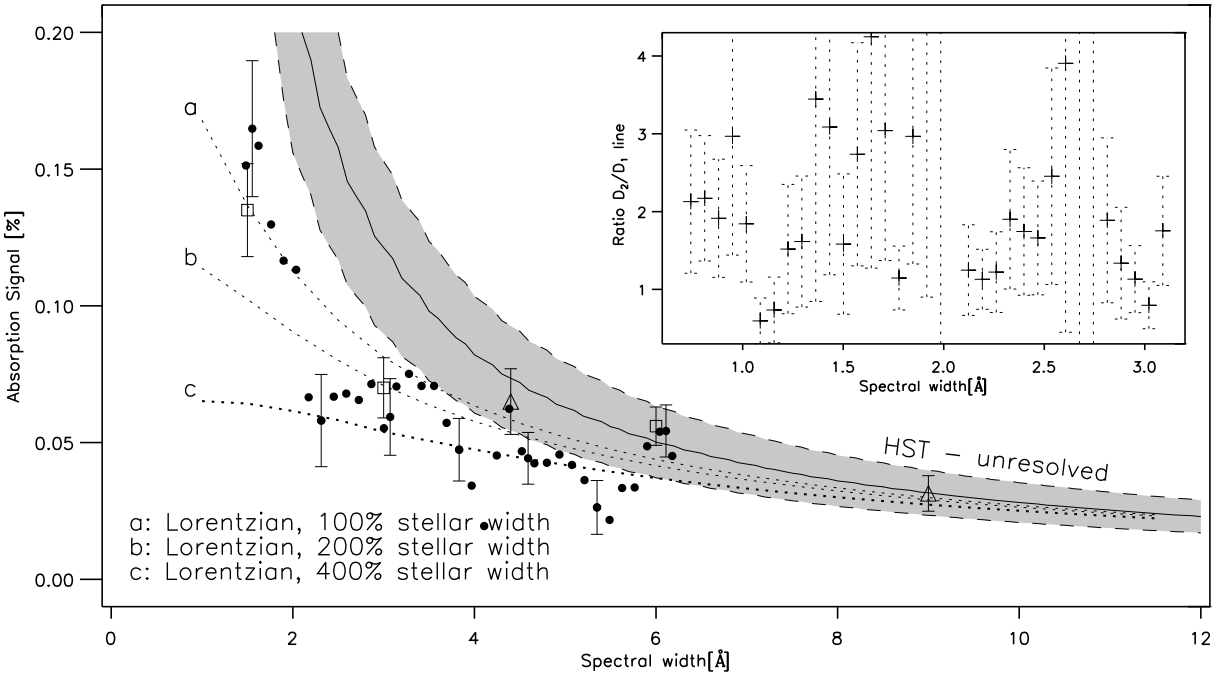

Figure 6.8 — Transmission spectroscopy around the Fraunhofer D line. The absorption signal in the two Na D lines is plotted over the total width of the central passbands. The filled circles indicate the average absorption in the D_1 and D_2 lines. Every tenth data point shows the 1-σ uncertainty. The open squares indicate the absorption signal found by Snellen et al. (2008) and the open triangles the absorption found by Sing et al. (2008a). The line indicates the absorption found by Charbonneau et al. (2002), if the absorption by the planetary line would be completely unresolved. The lines indicated by *a, b, c,* show the Na D absorption levels as a function of passband, expected from the HST measurements, assuming that the atmospheric absorption feature is Lorentzian shaped with a width equal to, 2× and 4× the stellar width of the Na D doublet. The insert shows the ratio of the depth of the absorption found in the D_2 and D_1 lines over the different band passes.

change in the relative radial-velocity a complete removal would be difficult and the fact that this line is always in the central passband means that it cannot introduce a systematic effect. Finally, the seeing changes over night (Figure 6.1), and the Rossiter-McLaughlin effect, which changes the shape of the absorption line during the transit, would further complicate a removal (see also the discussion in Snellen et al. (2008) on this subject and Chapters 4 and 5 for an in depth discussion of the Rossiter-McLaughlin effect).

6.3.2 Sodium results

The results for both methods of removal of the telluric water lines are shown, for the four passbands, in the second and third columns of Table 6.1. Both methods lines turn out to give similar results. The values agree in all four passbands with each other and with the literature values within their 1-σ uncertainties, with the exception of the values derived in the 4.4 Å passband. The latter value derived using the second method lies just outside the uncertainties of the literature value and the value derived using the first method. The correction coefficient

Table 6.1 — Comparison of the measurements of the sodium absorption by HD 209458b's atmosphere for the two different methods of correcting for the telluric water lines. The first column shows the result for which the correction for telluric water lines was carried out in the transmission spectroscopy and the second column shows the results for which the telluric water lines have been removed in the spectra and only a small additional correction was carried out. The values are given together with their 1-σ uncertainties, as derived from the χ^2 fit. The third and fourth columns show the results by Snellen et al. (2008) and Sing et al. (2008a).

Passband [Å]	This work		Snellen et al. (2008)	Sing et al. (2008a)
	Depth [%]			
1.5	0.151±0.025	0.129±0.025	0.135±0.017	
3.0	0.055±0.015	0.053±0.015	0.070±0.011	
4.4	0.062±0.011	0.044±0.011		0.065±0.012
6.0	0.052±0.010	0.042±0.010	0.056±0.007	

used to scale the telluric spectrum and the coefficient used in the former method to remove the influence of telluric lines correlate linearly, which is also expected. Furthermore we measured, using the latter method, the relative line strength of the sodium absorption in two passbands around the two Na D lines varying in width from 0.75 Å, to 3 Å in steps of 0.035 Å. The transit curves are shown in Figure 6.7 for the passbands of 0.75 Å, 1.5 Å, and 3 Å chosen to be similar to those in Snellen et al. (2008). The left panels show the absorption in the D_2 line, the middle panels in the D_1 line, and the right panels show the average of the two. All these measurements are also given in Table 6.1, and compared with the Snellen et al. (2008) and Sing et al. (2008a) results.

Instead of first conducting a fit only to the frames obtained outside of the transit, subsequently measuring and removing the telluric line contribution, and finally measuring the absorption depth, we also used the Levenberg-Marquardt least-squares minimization algorithm to simultaneously fit both the telluric line contributions and the transit depth. Both methods give similar results.

6.3.3 Potassium

Next to absorption by sodium, also absorption by potassium in the 7667 Å resonance doublet line is expected to be a prominent absorption feature in the transmission spectrum of hot giant planets (Seager & Sasselov 2000; Brown 2001). As the UVES observations cover the potassium lines at 7665 Å and 7699 Å, we searched for it in a similar way as for sodium. The potassium lines in our setting are located on the upper red CCD of the UVES spectrograph. Unfortunately, the line at 7665 Å overlaps with very strong telluric O_2 lines and we did not include it in our analysis. The wavelength region around the line at 7699 Å is shown in Figure 6.9.

To correct for the change in the blaze function of the spectrograph we used the same method as used before. As the spectral order immediately 'below' the order of interest is strongly effected by O_2 lines we used one order further away. This introduces a penalty of a slightly worse correction for the change in the blaze function.

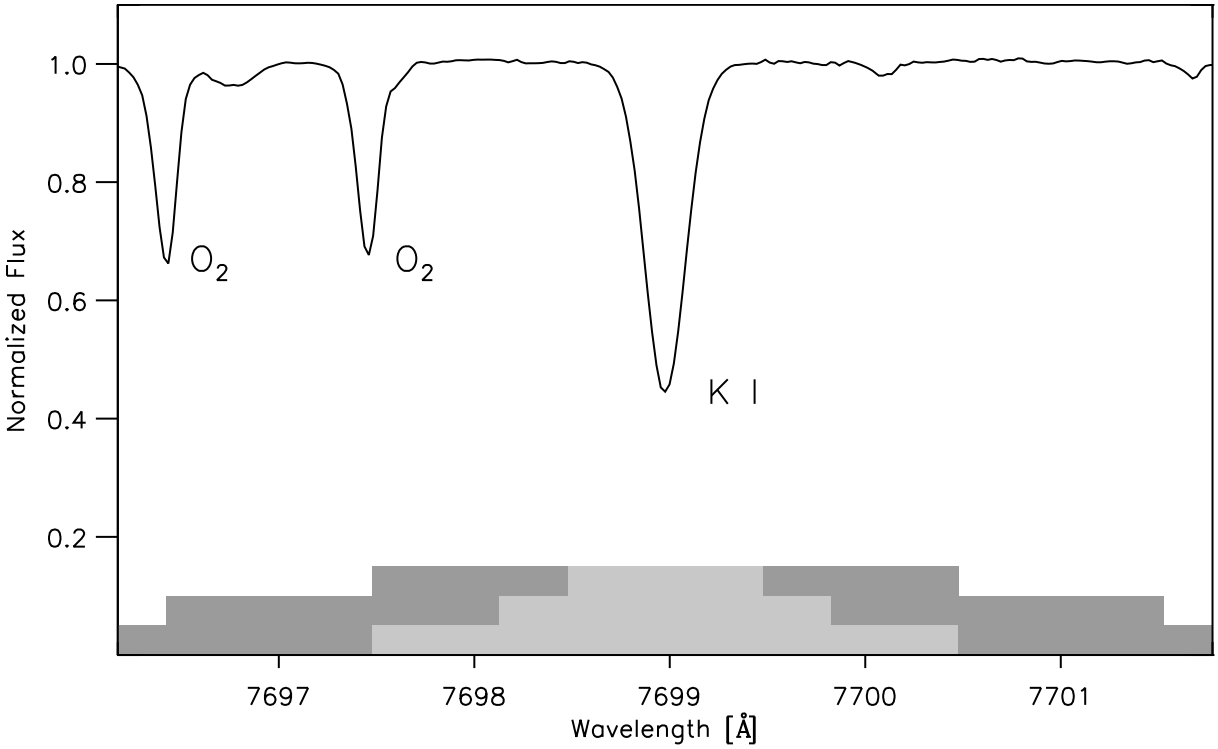

Figure 6.9 — The figure shows the spectral region around the K I line at 7699 Å, obtained with the UVES spectrograph. One can see two strong and a number of weaker telluric O_2 lines. Indicated by light gray areas are three central band-passes of 1 Å, 1.8 Å, and 3 Å, respectively. The dark gray areas indicate the sidebands.

The telluric contamination around the K I line is, besides that only one line can be used, less challenging. As expected, no absorption by telluric potassium is measured and the telluric O_2 lines in the spectral region of the K I line (Figure 6.9) follow the airmass nicely. We correct for the influence of the O_2 lines in the transmission spectroscopy after applying Equation 6.1 with a number of band-passes which have total widths between 0.4 Å and 4 Å. As in the case of the Na D lines we fit simultaneously for absorption during transit and contamination by O_2 lines.

Figure 6.10 shows the results obtained in the different band-passes. We find no significant absorption by the planetary atmosphere in the applied band-passes. In the band-passes with a width of 1.5 Å, and 2.5 Å we find 3-σ limits of 0.042%, and 0.015%, respectively. It is worth pointing out that our measurements only cover a narrow spectral band. If there exists an absorption feature by potassium which is broader than the widest band pass used here, than it would not be detected by our measurements.

Note the features at passbands of widths of $\sim$ 0.6 Å, $\sim$ 1 Å, $\sim$ 1.8 Å, and $\sim$ 3 Å, shown in Figure 6.10. These originate from the change in the wavelength position of the telluric absorption lines relative to the wavelength of the potassium absorption line over night. The sign of the derivations is positive if the telluric line moves out of the central band over the course of the night. The derivation is negative if the telluric line moves out of one of the side passbands. The signature at 3.0 Å for example originates from the movement of the telluric line at $\sim$ 7697.5 Å out of the central band (see Figure 6.9). Over the course of the night, the

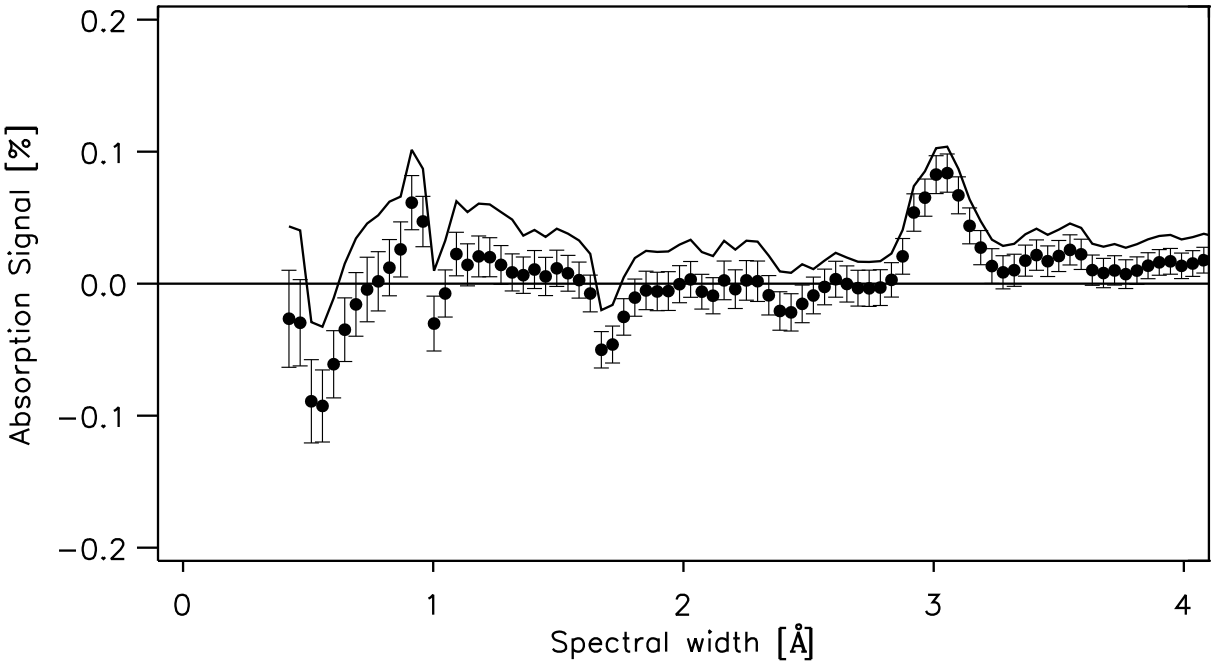

Figure 6.10 — Transmission spectroscopy around the potassium line at 7699 Å. The absorption signal is plotted over width of the central passband. Note that the width indicated here on the x-axis, is the width of one passband and not two as for the two Na D lines. The solid line shows the 3-σ line. See text for an explanation of the features at $\sim$ 0.6 Å, $\sim$ 1 Å, $\sim$ 1.8 Å, and $\sim$ 3 Å.

star gets red-shifted while the telluric line remains at its wavelength. This leads to extra flux in the central band and neither the transmission spectroscopy nor the correction for the O_2 lines applied here do correct for this effect. Normalizing the flux at the end of the night, when the absorption line was less present in the central passband will lead to an "extra absorption" in the central band during transit at the beginning of the night. If the telluric line is moving in a side band, like it is the case if the pass bands have widths of $\approx$ 1 Å and 1.8 Å, the effect is opposite. This is the same effect already described in section 6.3.1 in the context of the telluric lines around the Na D lines. For the feature at $\sim$ 0.6 Å a telluric O_2 line is responsible, which is located on one side of the potassium line and can not be easily seen in Figure 6.9. To minimize this effect and as no other correction need to be applied, we included only the first 35 frames obtained during the night in our analysis.

As indicated before, the upper limits derived in this section for the absorption by potassium in the K I resonance line are made using only one of the two potassium resonance lines. Note that due to spin coupling one would expected deeper absorption (by a factor of 2) in the potassium line not measured, if this ratio is not influenced by the planet's atmospheric environment.

6.4 Discussion

The absorption depths of sodium due to the planetary atmosphere measured in the UVES spectra are, within their uncertainties, consistent with the Subaru values of Snellen et al. (2008), and

the results by Charbonneau et al. (2002), and Sing et al. (2008a) (Table 6.1). Figure 6.8 shows our results (filled circles), the results by Snellen et al. (2008) (open squares), the results by Sing et al. (2008a) (open triangles), and as solid line and grey band, the HST measurement by Charbonneau et al. (2002) assuming it is completely unresolved within our passbands. In agreement with the results by Snellen et al. (2008) we find in this data set that it seems as if the Na D absorption lines in the planetary atmosphere are partly resolved out in the narrowest band passes, since they appear significantly below the expected absorption of the unresolved core. We over-plot the same lines that Snellen et al. (2008) have used in their Figure 5, *a, b, c,* which indicate the Na D absorption levels as a function of passband expected from the HST measurements, assuming that the atmospheric absorption feature is Lorentzian shaped with a width equal to, $2\times$ and $4\times$ the stellar width of the Na D doublet.

The correlated measurements of the sodium absorption for the different passbands show, as expected, no sudden change in absorption depth with the width of the band-pass. Considering the results shown here used passbands which differ only by four pixels, two on each side, so there is still a considerable amount of scatter in the data. The scatter in the absorption signal between adjacent passbands is due to different effects for narrow and wide passbands. For the smaller passbands the photon noise in the different pixels is the dominant source of scatter. For wider passbands the difference between the measured absorption signal is more correlated and might partly be due to residuals of the telluric spectrum or residual effects from the blaze function correction. See Figure 6.10 for comparison and section 6.3 for the explanation of these effects.

The stellar Na D_2 line shows more absorption by a factor of ~ 1.8 than the Na D_1 line. This confirms a trend already seen at lower resolution in the HST/STIS data (Sing et al. 2008b), but now also confirmed at a higher spectral resolution. Note that the ratio of the D_2/D_1 lines decreases for wider pass bands in our data (see insert in Figure 6.8). Further, it seems as if the results obtained by first removing the telluric lines in the spectrum lead to somewhat smaller values for the planetary absorption, as can be also seen in Table 6.1 in particular for wider band passes. This could for example originate from a imperfect match of the relative line strength of the telluric water lines a few ångström away from the Na doublet, to which we fitted the telluric spectra, and the telluric water lines which actually lie in one of the band passes. This might explain the decrease in the line ratio, which is not seen in the more noisy measurements without removal of the telluric contribution (not shown here).

It is interesting to note that for the Na D_2 line at mid transit, phase ~ 0, the absorption of the stellar starlight by the atmospheric sodium in HD 209458b seems to be weaker than before and after mid-transit. This effect can be seen over all passbands used for the D_2 line, but it is, due to the higher S/N in the detection of the sodium absorption, best seen in the narrow passbands. Figure 6.11 displays our results obtained for a passband of 0.75Å and the results by Snellen et al. (2008) using a passband of the same width which seem to display a similar effect. If this decrease in the apparent absorption by atmospheric sodium during mid-transit in the Na D_2 line is real, which certainly needs additional confirmation, one can speculate what can cause a decrease in the absorption by atmospheric sodium during mid-transit. The radial-velocity of the planet changes during the transit by ($\pm \sim 16\mathrm{km\,sec}^{-1}$). This corresponds to a shift in wavelength of $\pm \sim 0.3$ Å. If the cross-section of the sodium in HD 209458b atmosphere has a similar or smaller spectral width than the stellar sodium absorption lines, it will, at the beginning and end of the transit, mainly absorb light from the sides of the stellar absorption line. During mid-

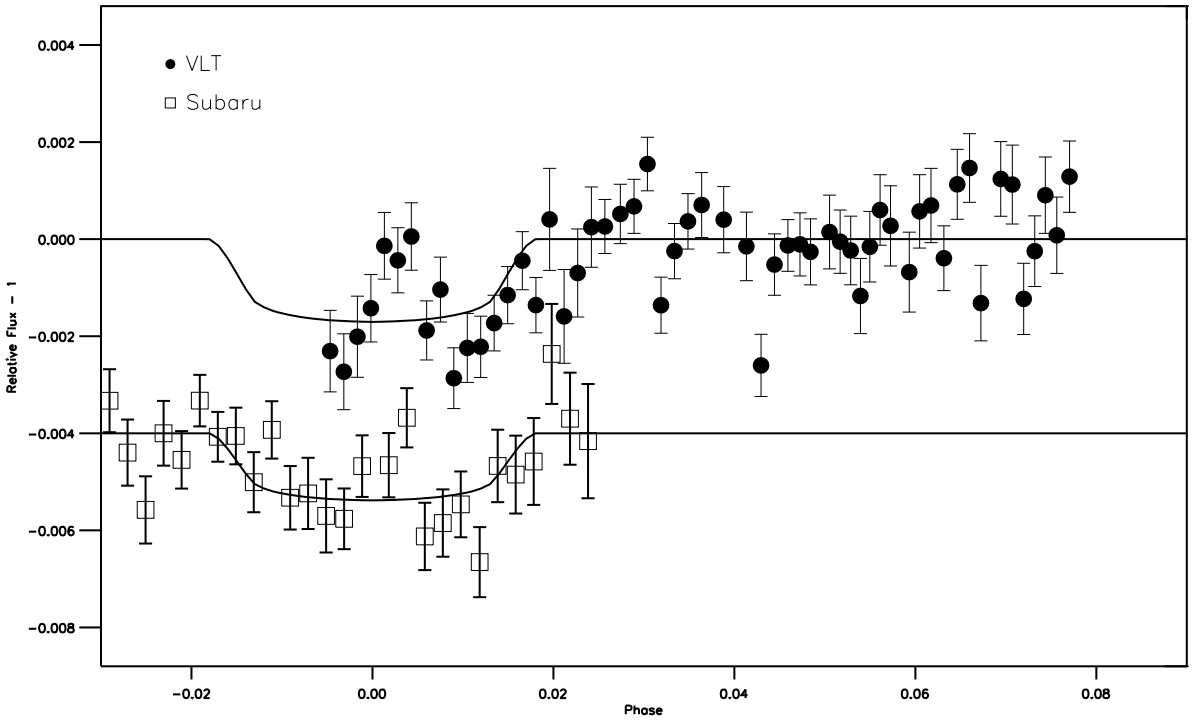

Figure 6.11 — Transmission spectroscopy of the Na D_2 line. The data points indicated by circles are obtained in this work using the UVES at the VLT. The data points indicated by squares are obtained using the HDS at the Subaru telescope. Both data sets show a possible decrease in the absorption around mid-transit, albeit at a low S/N level. The solid lines represent the best fits to the two data sets.

transit there will be only a small radial velocity difference between the star and planet. The two cores of the absorption lines, stellar and planetary, overlap and the planetary atmosphere mainly absorbs light from the core of the stellar absorption line where the intensity is already a factor of a few lower than in the wings and the surrounding continuum. As transmission spectroscopy measures only the change of flux in the total central band this would indeed produce a apparent reduction of absorption during mid-transit. To cause such an effect the planetary absorption line has to be narrow compared to the stellar line as the absorption due to the planetary sodium goes nearly back to zero during mid-transit. As the normalized intensity in the stellar absorption line drops form ~ 0.7 to ~ 0.1 over 0.3 Å it might however be possible that the change in radial-velocity of the planet during the transit indeed accounts for part of this effect. However, a very narrow planetary absorption line would not agree with our findings that the core of the planetary absorption line is partly resolved. In addition for the Na D_1 line a reduction of the absorption during mid-transit is not detected. It might however be missed as the overall level of absorption in this line is lower, and possibly changes in the atmospheric absorption with time are below the S/N ratio available in these measurements. In summary, the effect described here can not firmly be confirmed and characterized with this data set. However, the principle of this effect, changes in the measured absorption during a transit due to changes in radial-velocity of the planet, might open the possibility to further probe the structure of the atmospheric absorption lines. This however requires very high signal to noise observations with an evenly high control of systematic effects. Furthermore a change in the shape of the stellar absorption line

from center to limb might contribute to this effect (e.g. Pierce & Slaughter 1982).

That no potassium absorption by the planetary atmosphere has been measured is to some degree surprising, as models which predict planetary absorption in the line Na D doublet also predict absorption in the K I doublet (e.g. Seager & Sasselov 2000; Brown 2001). It does however fit together with the measurement of a lower than expected absorption of sodium by HST, which is confirmed by Snellen et al. (2008) and this work. Many explanations have been put forward to explain this, for example, by low sodium abundance, atmospheric circulation, high clouds, photo-ionization and others (see Seager 2003). Together with an upper limit for CO absorption by Deming et al. (2005), our upper limit for the K I line supports the idea that high clouds might be responsible for the low depth of the sodium absorption (Seager 2008). This further agrees with the findings of Snellen et al. (2008) and this work that the width of the sodium is comparable to the width of the stellar lines. High clouds would suppress the wings of the planetary absorption lines. Based on spectra from brown dwarfs, with similar T_{eff} as hot Jupiter's, it was thought that the alkali lines are very broad and span several nanometer (Seager & Sasselov 2000).

6.5 Conclusions

In this chapter we presented our results on the measurement of absorption by sodium and potassium in the Na D and K I lines, using the UVES spectrograph at ESO's Paranal observatory during planetary transit. We detect absorption by sodium consistent with earlier space and ground-based measurements. We further extend on these by measuring the ratio of the two Na D independently in a number of narrow wavelength bands. Our data also suggest a decrease of absorption in the D_2 line during mid-transit for which we have a tentatively explanation. With the same observations and same technique we establish an upper limit for absorption by potassium in the K I line, which makes us confident that this upper limit is reliable. These measurements support the idea that HD 209458b has high clouds.

Our results show that it is possible to observe atmospheric features of extra solar planets with earth based observatories, even under non-ideal observing conditions. The results form two data sets taken at different observatories under different weather conditions do not only agree with each other qualitatively, they also agree on a quantitative level. This is encouraging as it not only shows that transmission spectroscopy from the ground is reliable, it also appears as it is now feasible to probe the atmospheres of planets which are around stars one or two magnitudes fainter, or have a smaller relative coverage of the stellar surface or a smaller atmospheric scale height.

Acknowledgments

We would like to thank the support astronomer at ESO's Paranal observatory for his excellent support during the observations.

Bibliography

Brown, T. M. 2001, ApJ, 553, 1006 100, 110, 115
Charbonneau, D., Brown, T. M., Noyes, R. W., & Gilliland, R. L. 2002, ApJ, 568, 377 100, 109, 113
Dekker, H., D'Odorico, S., Kaufer, A., Delabre, B., & Kotzlowski, H. 2000, in Proc. SPIE, ed. M. Iye & A. F. Moorwood, Vol. 4008, 534 100
Deming, D., Brown, T. M., Charbonneau, D., Harrington, J., & Richardson, L. J. 2005, ApJ, 622, 1149 115
Lundstrom, I., Ardeberg, A., Maurice, E., & Lindgren, H. 1991, A&AS, 91, 199 102, 107
Mendillo, M. 2001, Earth Moon and Planets, 85, 271 105
Moutou, C., Coustenis, A., Schneider, J., et al. 2001, A&A, 371, 260 105
Patat, F. 2008, A&A, 481, 575 104
Pierce, A. K. & Slaughter, C. 1982, ApJS, 48, 73 115
Redfield, S., Endl, M., Cochran, W. D., & Koesterke, L. 2008, ApJ, 673, L87 100
Seager, S. 2003, in ASP Conference Series, Vol. 294, Scientific Frontiers in Research on Extrasolar Planets, ed. D. Deming & S. Seager, 457 115
Seager, S. 2008, Space Science Reviews, 135, 345 115
Seager, S. & Sasselov, D. D. 2000, ApJ, 537, 916 100, 110, 115
Sing, D. K., Vidal-Madjar, A., Desert, J. ., Lecavelier des Etangs, A., & Ballester, G. 2008a, ArXiv e-prints, 802 100, 107, 109, 110, 113
Sing, D. K., Vidal-Madjar, A., Lecavelier des Etangs, A., et al. 2008b, ArXiv e-prints, 803 100, 113
Snellen, I. A. G., Albrecht, S., de Mooij, E. J. W., & Le Poole, R. S. 2008, A&A, 487, 357 99, 100, 103, 107, 109, 110, 112, 113, 115
Winn, J. N., Suto, Y., Turner, E. L., et al. 2004, PASJ, 56, 655 103